Improved spatial resolution in time-resolved transillumination imaging using temporal extrapolation with the cumulant expansion solution to the transport equation

E. Ortiz-Rascón, N. C. Bruce, A. A. Rodríguez-Rosales, J. Garduño-Mejía and R. Ortega-Martínez
Centro de Ciencias Aplicadas y Desarrollo Tecnológico, Universidad Nacional Autónoma de México, Circuito Exterior, Ciudad Universitaria, Apartado Postal 70-186 México, D.F. 04510
E-mail: neil.bruce@ccadet.unam.mx

Received 7 June 2013; accepted 23 August 2013

This paper presents results of a time-resolved transillumination imaging method using temporal extrapolation. The temporal extrapolation is performed with the cumulant expansion solution to the transport equation. The results obtained are compared to results of the same method but using the diffusion approximation solution. It is found that the results are consistent but that the cumulant expansion method gives better resolution, by a factor of approximately 3, for the imaging process, because it gives a better estimation of the photon contribution for shorter integration times.

Keywords: Time-resolved imaging; laser imaging; tissue optics.

Este artículo presenta resultados de un método para la formación de imágenes resueltas temporalmente mediante la transmisión de luz usando una extrapolación temporal. La extrapolación temporal se realiza mediante la solución a la ecuación de transporte mediante la expansión en cumulantes. Los resultados obtenidos se comparan con los resultados del mismo método pero usando la solución mediante la aproximación de difusión. Se encuentra que los resultados son consistentes pero la el método usando la expansión en cumulantes da mejor resolución, en un factor de aproximadamente 3, para el proceso de formación de imágenes, esto debido a que da una mejor estimación de la contribución de los fotones con tiempos de integración menores.

Descriptores: Formación de imágenes resueltas temporalmente; formación de imágenes mediante láser; óptica de tejidos.

PACS: 87.63.lp; 87.63.lt; 87.64.Cc

1. Introduction

The study of the propagation of light in highly scattering media has many applications, particularly in the medical area [1,2], imaging of biological models [3] and characterization of materials [4]. In particular the technique of diffuse optical tomography (DOT) has been implemented in different configurations to study the structure of tissue [5-7]. To overcome the limitations of multiple light scattering inside tissue, DOT uses many source and detector positions to obtain experimental scattered light intensities and an inversion algorithm, typically using the diffusion approximation, to reconstruct the structure inside the sample from these measured boundary intensities. The spatial resolution of these methods is limited to about 4 mm at best [1,8,9]. This leads, in many cases, to the use of other imaging techniques, such as CT or MRI, simultaneously with the optical technique to provide high resolution images of the tissue structure [7]. In this paper we present an optical method which can be used to give complementary higher resolution information to improve a DOT image.

When illuminating a scattering sample with a pulse of light, intuitively, the light that emerges first from the sample has travelled the most direct path from the source to the detector and so can be used to form a shadow image. Different methods have been used to separate the directly-transmitted first-arrival-time photons from the remainder of the transmitted pulse. Kerr shutters [10], Raman amplifiers [11], and photorefractive techniques [12] are just some of the methods developed, as well as fast detectors [13-17] to separate the first few picoseconds of the transmitted pulse from the longer path-length photons. Using these methods the best resolution for an absorbing object in the centre of 50 mm of a tissue-like sample has been found to be approximately 10 mm [18].

Hebden and co-workers [18,19] showed that by fitting the detected experimental transmitted pulse to a theoretical curve, and then using the fitted curve, which has no experimental noise, to separate the first-arriving photons from the transmitted signal, the resolution for detection of absorbing objects at the centre of a 50 mm tissue-like sample could be improved to approximately 5 mm. In that work the diffusion approximation solution to the transport equation [20] was used as the fitting function and the authors reported that the same results were obtained by using the random walk solution [21]. It has also been shown that the inhomogeneities presents in tissue can cause very large variations in the early arriving light intensity meaning that the application of this type of method in medical applications is limited [22], however, the method of fitting a theoretical function to the detected pulse uses the light over a wide range of arrival times to extrapolate to the early photons, and should be less sensitive to this type of effect.

Cai and co-workers [23-27], in a series of papers, presented an alternative solution to the transport equation using the cumulant expansion method. They showed that their method gives improved results for short propagation times. It

is important to point out that this method is valid for a homogeneous sample, and so suffers from the same limitations as the methods used by Hebden *et al* [18,19], and in fact it is not obvious if the cumulant expansion method should give better results when used in the temporal extrapolation method. However, as will be shown below, this method does improve on the results presented by Hebden *et al* [18,19].

In the following section, the equations used for the fitting process, both for the cumulant expansion method, and the diffusion approximation method (as a comparison) are presented, the experimental set-up is described in Sec. 3, and the results are presented in Sec. 4. We give our conclusions in Sec. 5.

2. Theory

The diffusion approximation equation used to fit the experimental data of the transmitted intensity, $I\left(t,d\right)$, for a slab geometry as a function of time t and sample width d, on-axis, is the same as that used by Hebden *et al* [18,19], and is the equation derived by Patterson *et al* [20], given by Eq. (1):

$$\begin{aligned} I\left(t,d\right) = A\frac{1}{(4Dc\pi)^{3/2}}\frac{1}{(t-t_0)^{5/2}}\exp[-\mu_a c\left(t-t_0\right)] \\ \times\left\{\begin{array}{l} \left(d-z_0\right)\exp\left[-\dfrac{\left(d-z_0\right)^2}{4Dc\left(t-t_0\right)}\right] \\ -\left(d+z_0\right)\exp\left[-\dfrac{\left(d+z_0\right)^2}{4Dc\left(t-t_0\right)}\right] \\ +\left(3d-z_0\right)\exp\left[-\dfrac{\left(3d-z_0\right)^2}{4Dc\left(t-t_0\right)}\right] \\ -\left(3d+z_0\right)\exp\left[-\dfrac{\left(3d+z_0\right)^2}{4Dc\left(t-t_0\right)}\right] \\ +\left(5d-z_0\right)\exp\left[-\dfrac{\left(5d-z_0\right)^2}{4Dc\left(t-t_0\right)}\right] \\ -\left(5d+z_0\right)\exp\left[-\dfrac{\left(5d+z_0\right)^2}{4Dc\left(t-t_0\right)}\right] \end{array}\right\} \end{aligned} \quad (1)$$

where A is an arbitrary intensity factor, D is the diffusion coefficient given by $D=\left(1/3\right)\left(\mu_a+\mu_s'\right)^{-1}$, c is the speed of light in the sample medium, μ_a is the absorption coefficient, μ_s' is the transport scatter coefficient given by $\mu_s'=\mu_s\left(1-g\right)$ with μ_s the scatter coefficient and g the mean cosine of the scatter distribution (the average cosine of the scattering angle) of one scatter particle of the model sample, and z_0 is the reciprocal of the transport scattering coefficient. The parameter d is the width of the sample and t_0 is the parameter indicating the arrival time of the incident pulse on the sample.

The equivalent equation for the cumulant expansion method as derived by Cai *et al* is [23-27]

$$\begin{aligned} I(\mathbf{r},\mathbf{s},t) = A\Bigg[N(\mathbf{r},t)F(\mathbf{s},t) \\ -\frac{3}{4\pi}D(t-t_0)\,\mathbf{s}\cdot\nabla_{\mathbf{r}}N(\mathbf{r},t)\Bigg] \end{aligned} \quad (2)$$

where $I\left(\mathbf{r},\mathbf{s},t\right)$ is the photon distribution function depending on position $\mathbf{r}$, direction $\mathbf{s}$, and time t, with:

$$\begin{aligned} F(\mathbf{s},t) = \frac{1}{4\pi}\sum_l(2l+1) \\ \times\exp\left[-g_l\left(t-t_0\right)\right]P_l(\mathbf{s},\mathbf{s}_0) \end{aligned} \quad (3)$$

$$\begin{aligned} N(\mathbf{r},t) = \Bigg[N^{(0)}(\mathbf{r},t|x_0,y_0,z_0,\mathbf{s}_0) \\ -N^{(0)}(\mathbf{r},t|x_0,y_0,-z_0-2l_t,\mathbf{s}_0)\Bigg] \\ +\Bigg[N^{(0)}(\mathbf{r},t|x_0,y_0,z_0+2d,\mathbf{s}_0) \\ -N^{(0)}(\mathbf{r},t|x_0,y_0,-z_0+2d-2l_t,\mathbf{s}_0)\Bigg] \\ +\Bigg[N^{(0)}(\mathbf{r},t|x_0,y_0,z_0-2d,\mathbf{s}_0) \\ -N^{(0)}(\mathbf{r},t|x_0,y_0,-z_0-2d-2l_t,\mathbf{s}_0)\Bigg] \end{aligned} \quad (4)$$

$$\begin{aligned} N^{(0)}(\mathbf{r},t|\mathbf{r}_0,\mathbf{s}_0) = \frac{1}{\left[4\pi D(t-t_0)\,c\,(t-t_0)\right]^{3/2}} \\ \times\exp\left\{-\frac{\left[\mathbf{r}-\mathbf{r}_0-\mathbf{s}_0\,\Delta(t-t_0)\right]^2}{4D(t-t_0)\,c\,(t-t_0)}\right\} \\ \times\exp\left[-\mu_a c\,(t-t_0)\right] \end{aligned} \quad (5)$$

where $N^{(0)}\left(\mathbf{r},t|\mathbf{r}_0,\mathbf{s}_0\right)$ is the photon density for a point pulse propagating along $\mathbf{s}_0$ at position $\mathbf{r}_0=(x_0,y_0,z_0)$ and time t_0; which uses the transport mean free path l_t and the relations

$$g_l = c\,\mu_s\,\left(1-\frac{a_l}{2l+1}\right) \quad (6)$$

$$P\left(\mathbf{s},\mathbf{s}'\right) = \frac{1}{4\pi}\sum_l a_l P_l\left(\mathbf{s},\mathbf{s}'\right) \quad (7)$$

which is an expansion of the scattering phase function (which describes the fraction of light energy incident on a scattering particle from the $\mathbf{s}'$ direction that gets scattered into the $\mathbf{s}$ direction) in Legendre functions, and,

$$\Delta(t-t_0) = \frac{c\left\{1-\exp\left[-g_1\left(t-t_0\right)\right]\right\}}{g_1} \quad (8)$$

$$D(t-t_0) = \frac{c}{3(t-t_0)}\left\{\frac{(t-t_0)}{g_1} - \frac{1-\exp[-g_1(t-t_0)]}{g_1^2} - \frac{\{1-\exp[-g_1(t-t_0)]\}^2}{2g_1^2}\right\} \quad (9)$$

where $\Delta(t-t_0)$ is the average center of photons, which moves with speed c initially and stops at $c/g_1 = l_t$ in the long time limit [24], and $D(t-t_0)$ is the time-dependent diffusion coefficient. A full definition of these quantities can be found on Ref. 23. The equations for the cumulant expansion method were programmed in C using algorithms from the book "Numerical Recipes in C" [28] to verify that the calculation was correct. The results were compared to results published previously by Hebden and Delpy [19], for parameters $\mu_s = 9.07$ mm^{-1}, $g = 0.916$, $\mu_a = 0.011$ mm^{-1}, $c = 0.225$ mm ps^{-1} and $d = 51$ mm. Figure 1 shows the results of the cumulant expansion method for this case, which can be compared to Fig. 3 of Hebden and Delpy [19], to see the very good agreement between the results of the cumulant approximation with the experimental results of [19]. It is important to note that the cumulant expansion result is obtained using the experimentally measured values given above; there is no fit of the equation to the experimental data in this case.

The diffusion approximation, Eq. (1), was programmed in the commercial program Origin and the non-linear fitting algorithm in Origin was used to fit the experimental data for these cases. For the cumulant expansion method, Eqs. (2) - (9), a fitting program was written in C using the Levenberg-Marquardt method [28], due to the complexity of the equations involved, and was tested by generating a pulse with the cumulant expansion method, then using the fitting program to recover the original parameters used in the simulation. It was found that the values of the original parameters could be recovered with an error of less than 1%.

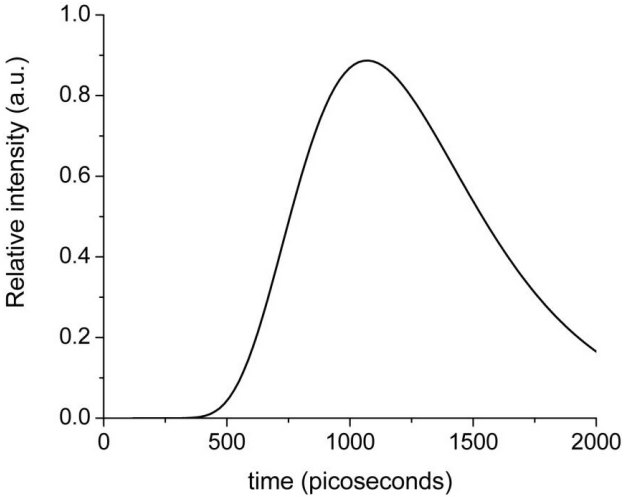

FIGURE 1.Result of calculation with the cumulant expansion method for a sample with parameters $\mu_s = 9.07$ mm^{-1}, $g = 0.916$, $\mu_a = 0.011$ mm^{-1}, $c = 0.225$ mm^{-1} and $d = 51$ mm, as reported by Hebden and Delpy [19].

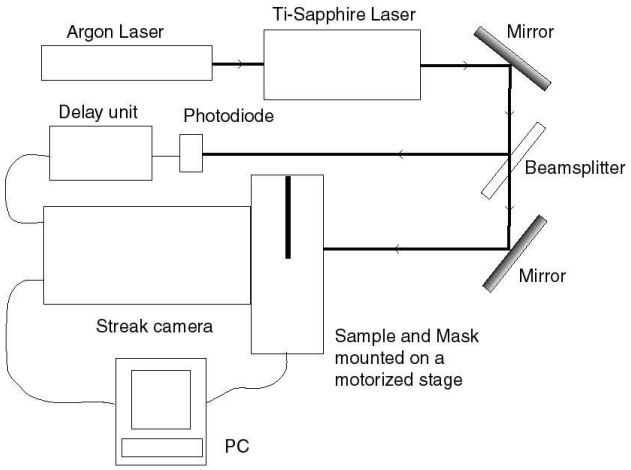

FIGURE 2. The experimental setup.

3. Experiment and Procedure

Figure 2 shows a schematic diagram of the experimental set-up. A Titanium-Sapphire laser (Coherent MIRA 900) pumped by an Argon ion laser (Coherent INNOVA 300) produces near bandwidth limited 200 fs pulses at 76 MHz repetition rate centered at 810 nm. The pulse width was measured by a second-order intensity autocorrelator and is much less than the temporal resolution of the streak camera (Hamamatsu Streakscope C10627) (about 42 ps sampling at the temporal range used). The pulses are divided by a beam splitter to generate a trigger signal (through a Hamamatsu Delay Unit C1097) and an incidence pulse on the sample. The intensity of the incidence pulse is controlled by filters to avoid saturating the streak camera. The incident beam is aligned with the centre of the streak camera entrance slit. The sample contains an absorbing mask (a black painted aluminium sheet) and the whole sample can be scanned across the beam (see Fig. 3).

The signal is detected and stored as a function of sample position. At each scan position of the mask the detected signal is averaged over 20 pixels of the streak camera output, which corresponds to an average over 125 μm, to reduce the noise in the pulse, and the fitting and further analysis of the data is performed on this averaged pulse. Samples of whole milk and diluted milk [29,30] were used in the results presented here.

Figure 4 shows a typical experimental curve obtained for one position of the mask. As reported by Hebden *et al* [18,19], to obtain a reasonable (in terms of the χ^2 parameter or the correlation parameter) fit it was necessary to use only part of the pulse to fit the theoretical equation. Depending on the parameters of the sample under test, for the cumulant expansion method and the diffusion method, fits of the pulse over a range of between 4 ns and 1 ns were used. The baseline (dark signal) values were removed before all the fitting processes were performed. In the fitting processes the

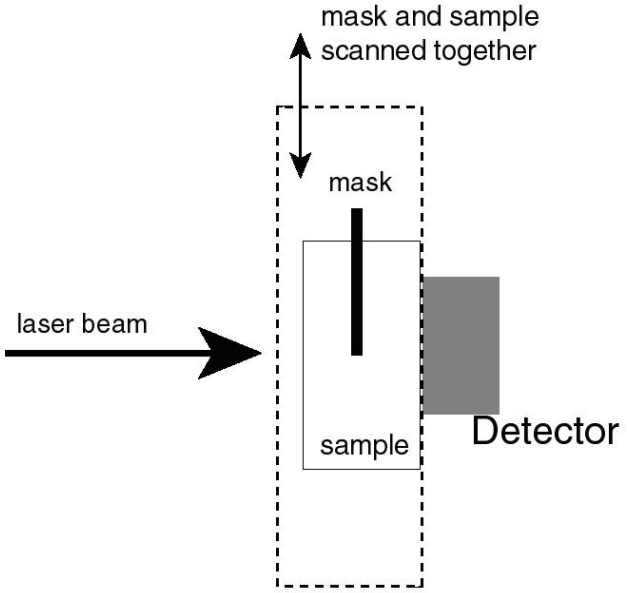

FIGURE 3. The sample and the mask are scanned together to cut the direct beam reaching the detector. The dotted rectangle corresponds to the motorized stage.

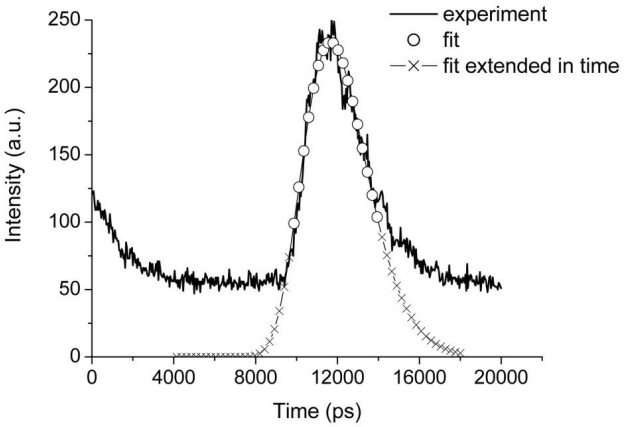

FIGURE 4. The result of fitting the cumulant expansion method to the experimental data. The graph shows an example of the fit for the case of whole milk.

parameter d (the sample width) was fixed to 50 mm, c (the speed of light in the sample medium) was set to correspond to a refractive index of 1.4, the parameter g was fixed at 0.9, and the value of t_0 was fixed from an experiment detecting the arrival time of the pulse without the sample and then correcting for the time of propagation through the sample to find the arrival time of the pulse on the front face of the sample, these values were $t_0 = 3.33$ ns for the diluted milk, and $t_0 = 5.33$ ns for the whole milk. The parameters adjusted in the fitting process are: μ_s, μ_a, and A. An example of the fit for a 50 mm wide sample of whole milk for a single position of the mask is shown in Fig. 4. In this case the fit was over a range of 4 ns, and the theoretical equation with the fit parameters was extended over a wider range to cover the part of the pulse where the experimental noise dominates.

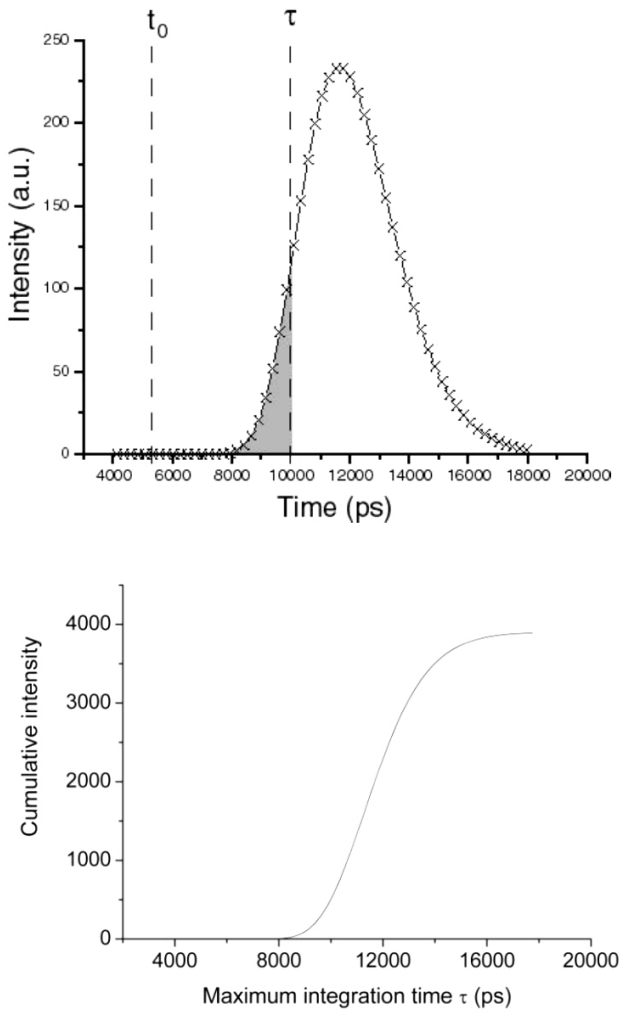

FIGURE 5. a) The cumulative intensity (shown in grey) of the extended fitted pulse (crosses) for a maximum integration time of τ; b) an example of the cumulative intensity function for one position of the mask.

The cumulative intensity, $I_c(\tau)$, of the extended fitted pulse, shown in the top graph of Fig. 5, is then calculated as a function of the upper limit, τ, of the time integral [18,19]

$$I_c(\tau) = \int_{t_0}^{\tau} I\,(t)\,\mathrm{d}t \tag{10}$$

This equation gives the intensity as a function of integration time, as shown in the bottom graph of Fig. 5. For a non-fluorescent and non-phosphorescent media the integration over the full duration of the transmitted pulse would give the same result as using a CW laser, and as the integration time τ decreases, shorter path lengths are considered and the resolution should improve. This operation is performed for all of the positions of the scan of the sample and mask across the incident beam, and the image of the edge as a function of τ is constructed (Fig. 6). Note that the bottom graph of Fig. 5 is a horizontal line in Fig. 6.

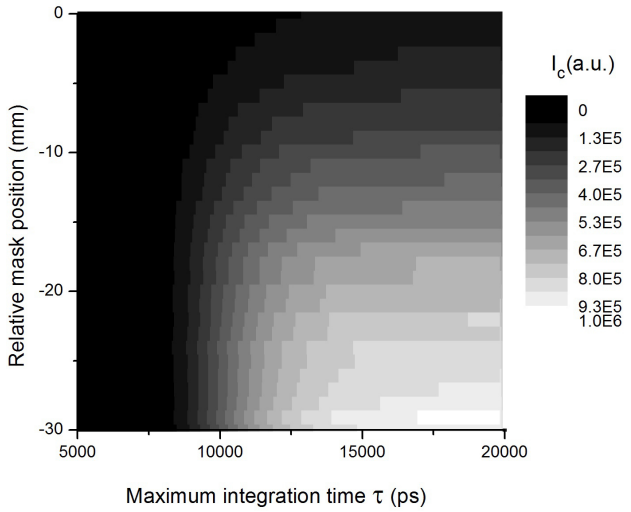

FIGURE 6. Graph of the value of $I_c(\tau)$ as a function of mask position.

Then, for each integration time τ, the image of the edge of the mask (a vertical cut of Fig. 6) is fit to the Bentzen [31] equation for the image of an edge assuming a Gaussian point spread function, *i.e.* the edge spread function, given by

$$E(y-y_0) = \frac{C_1}{2} + \frac{C_1}{2}\, erf\left(\frac{y-y_0}{\sigma\sqrt{2}}\right) + C_2 \qquad (11)$$

where C_1 and C_2 are fitting constants, $erf()$ is the error function, $y - y_0$ is the edge position and σ is a measure of the width of the region of the image where the intensity is changing. The parameter σ can also be related to the resolution of the imaging process, and the resolution is given by: $R = 2.93\sigma$, using the criterion used by Hebden *et al* [18,19], of 10% of the maximum MTF value.

4. Results

Figures 7 and 8 show the results of the resolution values obtained for two different samples; 50 mm wide samples of whole milk and diluted milk (33% milk, 67% water), respectively.

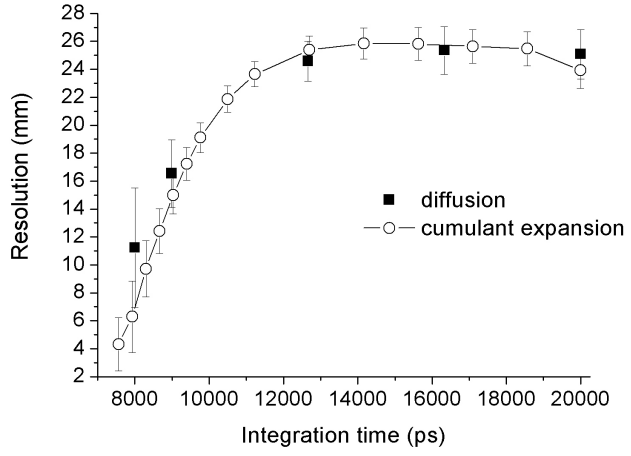

FIGURE 7. The value of the resolution limit as a function of integration time for whole milk.

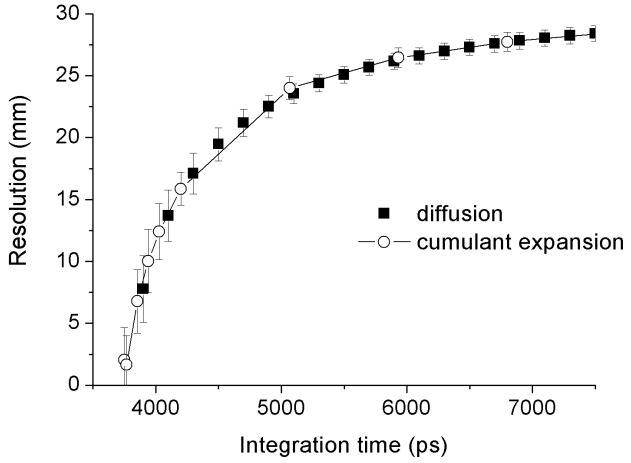

FIGURE 8. The value of the resolution limit for diluted milk (33% milk, 67% water).

The fitted values for the samples with no mask were, for the whole milk $\mu_a = 0.0026 \pm 0.0001$ mm^{-1} and $\mu_s' = 3.5417 \pm 0.0004$ mm^{-1}; and for the diluted milk $\mu_a = 0.0009 \pm 0.0001$ mm^{-1} and $\mu_s' = 1.0639 \pm 0.0001$ mm^{-1}. It should be noted that, for the diluted milk, the value of μ_s' is a typical value for tissue and is close to the value used by Hebden et al [18,19], whereas the value of μ_a is a factor of 10 lower than tissue and the value used by them. However, comparing the resolution values obtained with the diffusion method by Hebden *et al* [18,19], with the values reported here for the same method, the results are consistent (4.8 ± 2.5 mm compared to 7.5 ± 2.5 mm). From the figures it can be seen that, while the resolution values are very similar for the fit of the diffusion equation and the cumulant expansion results, the latter method allows results to be obtained for smaller integration times, thus improving the resolution obtained by a factor of approximately 3 (7.5 ± 2.5 mm for the diffusion method compared to 2.01 ± 2.58 mm).

Figure 9 shows the edge spread functions for values of τ near the limiting values for cases of fits to the cumulant method and to the diffusion method. Note that for similar values of τ the two methods give very different values of the intensity (the y-axes in these graphs), with the diffusion fit values being more than an order of magnitude smaller than the cumulant fit values. The fits to the theoretical edge spread function, Eq. (11), are also shown, except for the case of the diffusion fit for $\tau = 3800$ ps (Fig. 9(e)) where, because of the poor contrast, the noise and the increase of the intensity to the right of the apparent edge position, the result of the fit of Eq. (11) depends on the initial values of the parameters in the fitting algorithm. This means that the results of the fit are not reliable and cannot be reported. In fact, in some cases the value of σ obtained when fitting Eq. (11) to this case turned out to be negative. This case can be compared to the cumulant fit case (Fig. 9(b)) which is for a smaller integration time $\tau = 3766$ ps but still gives a stable and repeatable value for the fit to Eq. (11).

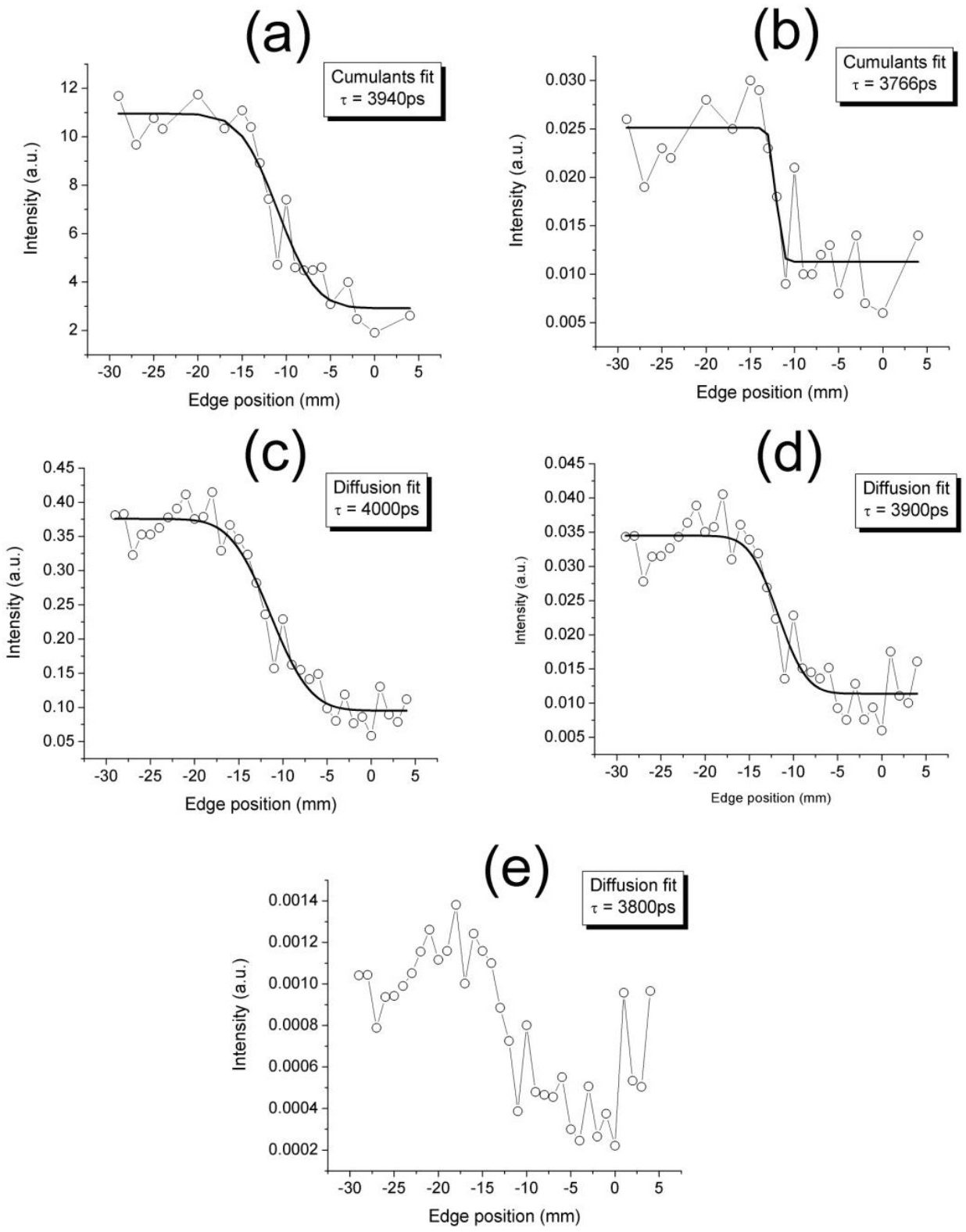

FIGURE 9. The edge spread functions for diluted milk obtained from the reconstructed pulses using a fit of the cumulant expansion method (a) and (b), and the diffusion approximation method (c), (d) and (e). The lines with the open circles are the edge spread function from the fitting methods, and the dark lines are the fits to Eq. (10).

5. Conclusions

In this paper we have shown an improvement in the temporal-extrapolation method for the detection and formation of images of absorbing objects inside scattering media. The improvement of approximately a factor of 3 in the resolution over previously reported results comes from the use of the cumulant expansion method solution to the transport equation. This result is important because it shows that with different fitting equations the results can be substantially improved. In particular it is interesting to note that the cumulant expansion method gives results which are better than the diffusion approximation for early photons. However it should be noted that it is not clear what the criteria for choosing a "better" fitting method are since in the cases presented here, both methods are valid for homogeneous media, which is not the case in the experiment with an absorbing object inside the scattering medium. It has been shown that the results obtained with the cumulant expansion method are consistent with the results of the diffusion method, and that the improvement comes from the ability to use shorter integration times with the cumulant expansion method. These results could be used to complement other DOT methods.

Acknowledgements

This work was partially supported by the Instituto de Ciencia y Tecnología del Distrito Federal (ICYTDF). Eduardo Ortiz-Rascón is grateful to the Universidad Nacional Autónoma de México (UNAM) for a doctoral grant.

1. T. Durduran, R. Choe, W. B. Baker, and A. G. Yodh, *Rep. Prog. Phys.* **73** (2010) 076701.
2. A. P. Gibson, J. C. Hebden, and S. R. Arridge, *Phys Med Biol.* **50** (2005) R1-R43.
3. A. Bassi, L. Fieramonti, C. D'Andrea, M. Mione, and G. Valentini, *J. Biomed. Opt.* **9** (2011) 100502-1.
4. C. D'Andrea, A. Nevin, A. Farina, A. Bassi, and R. Cubeddu, *Appl. Opt.* **48** (2009) B87-B93.
5. P. Taroni, G. Danesini, A. Torricelli, A. Pifferi, L. Spinelli, and R. Cubeddu, *J. Biomed. Opt.* **9** (2004) 464-473.
6. G. M. Turner, G. Zacharakis, A. Soubret, J. Ripoll, V. Ntziachristos, *Opt. Lett.* **30** (2005) 409-411.
7. R. Choe *et al*, *J. Biomed. Opt.* **14** (2009) 024020.
8. S. D. Konecky, G. Y. Panasyuk, K. Lee, V. Markel, A. G. Yodh, and J. C. Schotland, *Opt. Exp.* **16** (2008) 5048-5060.
9. D. Grosenick *et al*, *Appl. Opt.* **42** (2003) 3170-3186.
10. L. Wang, P. Ho, C. Liu, G. Zhang, and R. R. Alfano, *Science* **253 (**1991) 769-771.
11. M. D. Duncan, R. Mahon, L. L. Tankersley, and J. Reintjes, *Opt. Lett.* **17** (1992) 958-960.
12. S. C. W. Hyde, N. P. Parry, R. Jones, J. C. Dainty, P. M. W. French, M. B. Klein, and B. A. Wechsler, *Opt. Lett.* **20** (1995) 1331–1333.
13. G. Mitic, J. Kölzer, J. Otto, E. Plies, G. Sölkner, and W. Zinth, *Appl. Opt.* **33** (1994) 6699.
14. J. C. Hebden *Med. Phys.* **19** (1992) 1081-1087.
15. A. Andreoni, L. Nardo, G. Zambra, and M. Bondani, *J. Mod. Opt.* **56** (2009) 413-421.
16. L. Nardo , A. Brega, M. Bondani, and A. Andreoni, *Appl. Opt.* **47** (2008) 2477-2485.
17. A. Andreoni, L. Nardo, A. Brega, and M. Bondani, *J. Appl. Phys.* **101** (2007) 024921.
18. J. C. Hebden, D. J. Hall, and D. T. Delpy, *Med. Phys.* **22** (1995) 201-208.
19. J. C. Hebden and D. T. Delpy, *Optics Letters* **19** (1994) 311-313.
20. M. S. Patterson, B. Chance, and B. C. Wilson, *Appl. Opt.* **28** (1989) 2331-2336.
21. A. H. Gandjbakhche, G. H. Weiss, R. F. Bonner, and R. Nossal, *Phys. Rev. E* **48** (1993) 810-818.
22. A. H. Gandjbakhche, R. Nossal, and R. F. Bonner, *Med. Phys.* **21** (1994) 185-191.
23. W. Cai, M. Lax, and R. R. Alfano, *Phys. Rev. E* **61** (2000) 3871-3876.
24. M. Xu, W. Cai, M. Lax, and R. R. Alfano, *Opt. Lett.* **26** (2001) 1066-1068.
25. W. Cai, M. Xu, M. Lax, and R. R. Alfano, *Opt. Lett.* **27** (2002) 731-733.
26. W. Cai, M. Xu, and R. R. Alfano, *IEEE J. Sel. Tops. Quant. Electron.* **9** (2003) 189-198.
27. M. Xu, W. Cai, M. Lax, and R. R. Alfano, *Phys. Rev. E* **65** (2002) 066609-1.
28. W. H. Press, S. A. Teukolsky, W. T. Vetterling, and B. P. Flannery, in *Numerical Recipes in C: The Art of Scientific Computing, Second Edition* (Cambridge: Cambridge University Press, 2002).
29. K. J. Jeon, K. H. Lee, U. Kim, S. H. Park, G. Yoon, H. S. Eom, and D. Kim, *JKPS* **32** (1998) 823-827.
30. G. Mitic, J. Kolzer, J. Otto, E. Plies, G. Solkner, and W. Zinth, *Appl. Opt.* **33** (1994) 6699–6710.
31. S. M. Bentzen, *Med. Phys.* **10** (1983) 578-581.